

See discussions, stats, and author profiles for this publication at: <https://www.researchgate.net/publication/24279014>

Thioflavin T as a Molecular Rotor: Fluorescent Properties of Thioflavin T in Solvents with Different Viscosity

ARTICLE in THE JOURNAL OF PHYSICAL CHEMISTRY B · JANUARY 2009

Impact Factor: 3.3 · DOI: 10.1021/jp805822c · Source: PubMed

CITATIONS

109

READS

218

6 AUTHORS, INCLUDING:



[Vitali I Stsiapura](#)

University of Virginia

17 PUBLICATIONS 640 CITATIONS

[SEE PROFILE](#)



[Alexander Alexander Maskevich](#)

Yanka Kupala State University of Grodno

39 PUBLICATIONS 600 CITATIONS

[SEE PROFILE](#)



[Vladimir N Uversky](#)

University of South Florida

656 PUBLICATIONS 33,873 CITATIONS

[SEE PROFILE](#)

Article

**Thioflavin T as a Molecular Rotor: Fluorescent Properties
of Thioflavin T in Solvents with Different Viscosity**

Vitali I. Stsiapura, and Alexander A. MaskevichValery A. KuzmitskyVladimir
N. UverskyIrina M. Kuznetsova, and Konstantin K. Turoverov

J. Phys. Chem. B, **2008**, 112 (49), 15893-15902 • DOI: 10.1021/jp805822c • Publication Date (Web): 14 November 2008

Downloaded from <http://pubs.acs.org> on December 22, 2008

More About This Article

Additional resources and features associated with this article are available within the HTML version:

- Supporting Information
- Access to high resolution figures
- Links to articles and content related to this article
- Copyright permission to reproduce figures and/or text from this article

[View the Full Text HTML](#)



ACS Publications
High quality. High impact.

The Journal of Physical Chemistry B is published by the American Chemical Society, 1155 Sixteenth Street N.W., Washington, DC 20036

Thioflavin T as a Molecular Rotor: Fluorescent Properties of Thioflavin T in Solvents with Different Viscosity

Vitali I. Stsiapura* and Alexander A. Maskevich

Department of Physics, Yanka Kupala State University, Grodno 230023, Belarus

Valery A. Kuzmitsky

B.I. Stepanov Institute of Physics, National Academy of Sciences of Belarus, Minsk 220072, Belarus

Vladimir N. Uversky

Department of Biochemistry and Molecular Biology, Indiana University School of Medicine, Indianapolis, Indiana 46202

Irina M. Kuznetsova and Konstantin K. Turoverov

Institute of Cytology, Russian Academy of Sciences, St. Petersburg 194064, Russia

Received: July 2, 2008; Revised Manuscript Received: September 19, 2008

The effect of solvent viscosity on thioflavin T (ThT) fluorescent properties is analyzed to understand the molecular mechanisms of the characteristic increase in ThT fluorescence intensity accompanying its incorporation into the amyloid-like fibrils. To this end, the dependencies of the ThT quantum yield and fluorescence lifetime on temperature and glycerol content in the water–glycerol mixtures are studied. It has been found that fluorescent properties of ThT are typical for the specific class of fluorophores known as molecular rotors. It has been established that the low ThT fluorescence intensity in the solvents with low viscosity is caused by the nonradiative deactivation of the excited state associated with the torsional motion of the ThT benzthiazole and aminobenzene rings relative to each other, which results in the transition of ThT molecule to nonfluorescent twisted internal charge transfer (TICT) state. The rate of this process is determined by the solvent viscosity, whereas the emission does occur from the nonequilibrium locally excited (LE) state. High polarization degree of the ThT fluorescence ($P = 0.45$) observed for glycerol solutions of different viscosity confirms the nonequilibrium character of the emission from the LE state and testifies that rotational correlation time of the whole molecule is considerably greater than the time required to accomplish transition to the nonfluorescent TICT state. Torsional movements of the ThT fragments take place in the same temporal interval as solvent relaxation, which leads to nonexponential fluorescence decay of the dye in viscous solvents. This photophysical model successfully explains the fluorescent properties of ThT in solvents with different viscosities. The model is confirmed by the results of the quantum-chemical calculations, which showed that energy minimum for the ground state of ThT corresponds to conformation with torsional angle $\varphi = 37^\circ$ between the benzthiazole and aminobenzene rings and in the excited-state twisted conformation of ThT with $\varphi = 90^\circ$ has minimal energy. These data support the idea that the reason for the characteristic increase in the ThT fluorescence intensity accompanying its incorporation into the amyloid fibrils is determined by the rigidity of the dye environment, which prevents the rotation of the benzthiazole ring relative to the aminobenzene ring in the excited state.

Several human diseases (e.g., Alzheimer's and Parkinson's diseases, late-onset diabetes, etc.) are closely related to formation and deposition of amyloid fibrils—insoluble filamentous aggregates of proteins.^{1–7} One of the most frequently used methods of amyloid fibrils detection is based on the characteristic changes in thioflavin T (ThT) fluorescence intensity upon binding of this dye to amyloid fibrils.^{8–15} Importantly, ThT interaction with amyloid fibrils was reported^{8,10} to be highly specific, since addition of the dye to solutions of proteins in folded, unfolded, or partially folded monomeric forms was not accompanied by changes in the emission intensity. Therefore, due to these unique

properties, ThT represents a useful and convenient tool for the fast and reliable diagnostics of the presence of amyloid fibrils in disease-affected tissues and organs. Furthermore, in the *in vitro* fibrillation studies, the appearance of the specific ThT fluorescence is considered as an indication of the amyloid fibril formation.^{16–19} This approach is widely accepted, and the number of studies relying on the ThT diagnostic capabilities is rapidly growing. However, the molecular mechanisms of the specific ThT binding to amyloid fibrils and the reasons underlying the characteristic increase in the ThT fluorescence quantum yield accompanying the incorporation of this dye into the fibrils are poorly understood until now.

Several possible explanations of ThT fluorescence properties were reviewed.²⁰ Change of ThT emission intensity upon

* Corresponding author: phone +375-152-743414; Fax +375-152-731910; e-mail stepuro@grsu.by.

incorporation into amyloid fibrils was attributed to formation of highly fluorescent dimers,^{21–23} excimers,²⁴ and even micelles²⁵ from dye molecules. These hypotheses are based mainly on the data about significant red shift of fluorescence excitation and emission spectra upon ThT binding to fibrils. According to LeVine,¹⁰ aqueous solution of ThT is characterized by excitation and emission spectra with maxima located at 385 and 445 nm, respectively, while ThT bound to fibrils possesses excitation band near 450 nm and the emission at 482 nm. However, the reported spectral properties for ThT in aqueous solution are questionable, since its absorption spectrum has a maximum at 412 nm and does not correspond to the fluorescence excitation spectrum.²⁶ This fact testifies that the emission at 445 nm found for the free ThT in aqueous solutions originates from fluorescent impurities. Another weak point of these hypotheses is a low probability of dimerization or aggregation of ThT due to positive charge of the dye, and one can expect that electrostatic repulsion will prevent formation of dimers and micelles, particularly in nonpolar environment of fibrils.

On the other hand, it was reported that quantum yield (QY) of ThT fluorescence depended mainly on viscosity rather than on polarity or protic properties of solvents,^{26–28} and growth of viscosity or rigidity of microenvironment resulted in significant QY increase. It has been suggested that photoinduced intramolecular charge transfer takes place for the fluorophore,^{28,29} and ThT behaves as a molecular rotor.^{27–30}

The most prominent feature of the compounds referred to as molecular rotors^{31–36} is the significant fluorescence increase upon introduction into high-viscosity media due to the decreased torsional relaxation in the molecule. Internal rotation of molecular groups or fragments is associated with intramolecular charge transfer process,^{35,36} leading to transition from the fluorescent locally excited (LE) state to the nonfluorescent twisted internal charge transfer (TICT) state.

Detailed quantum-chemical calculations of the ground and excited states of ThT confirmed the applicability of this model to describe the dye photophysics.²⁹ It was found that internal rotation of benzthiazole and dimethylaminobenzene fragments in the excited singlet state was related to intramolecular charge transfer process and formation of nonfluorescent TICT state. It was suggested that the major factor determining the high quantum yield of the fibril-incorporated ThT is the steric restriction of the benzthiazole and aminobenzene rings rotation relative to each other. The main aim of the current work was to test this hypothesis, and the effect of solvent viscosity and temperature on ThT fluorescence in glycerol and water–glycerol mixtures was investigated. These experimental studies were supported by the quantum-chemical calculations of the ThT molecule and its derivative 2-(4'-(dimethylamino)phenyl)-6-methylbenzothiazole (BTA-2).

Materials and Methods

Materials. ThT samples from Sigma-Aldrich and Fluka (Switzerland) were analyzed in distilled water, glycerol (Merck, Germany), and 2-propanol (Baker). Glycerol concentrations in water–glycerol mixtures were measured using the Abbe refractometer (LOMO, Russia). Viscosity of the glycerol–water mixtures was estimated based on the glycerol concentrations. The temperature dependence of the viscosity of different glycerol solutions was taken from the literature.³⁷

Measurements of Steady-State and Time-Resolved Fluorescence. Absorption spectra were analyzed using Specord 200 PC (Analytik Jena, Germany) spectrophotometer. Fluorescence emission and excitation spectra were measured using the

CM2203 spectrofluorometer (Solar, Belarus). Fluorescence quantum yields were measured relative to coumarin 1 ($\Phi = 0.73$) in ethanol.³⁸

Time-resolved fluorescence measurements were performed using time-correlated single photon counting (TCSPC) technique. The samples were excited at 408 nm by picosecond laser PDL 800B (Picoquant, Germany) generating excitation pulses with typical half-widths of 70 ps. A TCSPC board TimeHarp 200 (Picoquant, Germany) was used for data acquisition, and decay curves were measured with 36 ps per channel discretization. The ratio of STOP to START pulses was kept $\leq 3\%$ to ensure good statistics. The overall width of instrument response function was about 300 ps, but applying deconvolution data analysis we were able to reach time resolution of better than 100 ps.

Analysis of the Fluorescence Decay Curves. Fluorescence decay curves were analyzed using a set of programs developed in Grodno State University³⁹ on the basis of the Marquardt nonlinear least-squares method.^{40,41} Fluorescence decay parameters were determined by the minimization of the functional χ^2 , which characterized the deviation of the calculated function $I(t_i)$ from the experimental decay curve $I_{\text{exp}}(t_i)$:

$$\chi^2 = \frac{1}{N} \sum_{i=1}^N W_i [I_{\text{exp}}(t_i) - I(t_i)]^2 \quad (1)$$

where W_i is weight factor and N is total number of experimental points. $I(t_i)$ was obtained by the convolution of decay law function $F(t)$ with the instrument response function $L(t)$:⁴¹

$$I(t) = \int_0^t L(t')F(t - t') dt' \quad (2)$$

We used two models of decay law function $F(t)$ to describe ThT fluorescence kinetics. In the first model $F(t)$ was represented as a linear combination of up to four exponentials

$$F(t) = \sum_j \alpha_j \exp\left(-\frac{t}{\tau_j}\right) \quad (3)$$

where α_j and τ_j are the amplitude and lifetime of the j th decay component, respectively. Weights S_j of the exponential components in the emission were calculated as $S_j = (\alpha_j \tau_j) / (\sum_k \alpha_k \tau_k)$. Averaged lifetimes for multiexponential decays were calculated according to the expression

$$\langle \tau \rangle = \frac{\sum_j \alpha_j \tau_j^2}{\sum_j \alpha_j \tau_j} = \frac{\sum_j \tau_j S_j}{\sum_j S_j} \quad (4)$$

It is well-known^{42,43} that fluorescence decay $F(t)$ of systems with significant structural or relaxational heterogeneity (proteins, fluorophores in rigid matrixes or viscous media, etc.) could not be adequately described in the framework of multiexponential model with a few components (eq 3).

Certainly, adding more exponentials to the fitting function, one can obtain quite a good description of decay kinetics, but, however, the physical meaning of parameters α_j and τ_j is usually lost. For such cases it was suggested⁴² to represent decay law $F(t)$ not with a set of exponentials but with a function

$$F(t) = \int_0^\infty \alpha(\tau) \exp[-t/\tau] d\tau \quad (5)$$

where $\alpha(\tau)$ describes the lifetime distribution of emitting centers.

However, recovery of the $\alpha(\tau)$ function in contrast to determination of multiexponential decay parameters (see eq 3) is more difficult since a large number of distributions can fit the data equally well. To find the solution of this ill-conditioned problem,⁴⁴ one needs to parametrize $\alpha(\tau)$ (for example, as a set of Gaussian distributions^{45,46}) or use regularization methods⁴⁷ if no a priori information about functional form of $\alpha(\tau)$ is known.

In this work we used the first approach; i.e., $\alpha(\tau)$ was represented as a series of Gaussian distributions:⁴⁶

$$\alpha(\tau) = \sum_{i=1}^n \alpha_i \exp(-(\tau - \tau_{0,i})^2/2\sigma_i^2) \quad (6)$$

where α_i , $\tau_{0,i}$, and σ_i^2 are the parameters of i th Gaussian distribution. For cases when $\tau_{0,i} < 3\sigma_i$, the truncated Gaussian distribution was used; i.e., the function $\alpha(\tau)$ was set equal to 0 for $\tau \leq 36$ ps (one channel unit).

To simplify the search for the fitting parameters, the continuous distribution $\alpha(\tau)$ was approximated as a sum of the large number of exponents.⁴⁸ In this representation, the decay function is described by the following equation:^{40,41,49}

$$F(t) = \sum_{m=1}^N \sum_{i=1}^n \frac{\alpha_i}{\sqrt{2\pi}\sigma_i} \exp\left[-\frac{(\tau_{0,i} - \tau_m)^2}{2\sigma_i^2}\right] \exp\left(-\frac{t}{\tau_m}\right) \quad (7)$$

where N is the division number of $\alpha(\tau)$ function. The parameters α_i , $\tau_{0,i}$, and σ_i of the function $F(t)$ were determined using the Marquardt nonlinear least-squares method.^{40,41,49} The Durbin–Watson parameter⁴¹ (DW), χ^2 , visual inspection of weighted residuals distribution $R(t)$, and autocorrelation function of residuals $C(t)$ were used as criteria to evaluate success of the fit.^{41,50}

Quantum-Chemical Calculations. Ab initio methods (basis set 6-31G) were used to calculate geometry of ThT cation ($Z = +1$) and its analogue 2-(4'-(dimethylamino)phenyl)-6-methylbenzothiazole (BTA-2) in the ground S_0 state (Figure 1). In order to obtain energies of the excited states for a given geometry, the semiempirical method INDO/S⁵¹ was used.

All calculations (with the exception for INDO/S) were performed using the PC GAMESS 7.0⁵² version of the set of quantum-chemical programs Gamess-US.⁵³ The energies of the excited states, charge transfer probabilities, and the oscillator strengths of the electronic transitions were calculated using a set of programs developed by one of us (V.A.K.). All calculations were performed for the molecules in the gas phase. Conformers geometries and the molecular orbitals were visualized using the Molekel program.⁵⁴

Results and Discussion

Quantum-Chemical Analysis of ThT Properties in the Ground and Excited States. Here we present a brief description of the results of the quantum-chemical calculations of ThT in the ground and excited singlet states. More detailed data can be found in ref 29. Figure 1 represents the ThT structure and shows that the molecule can be divided on three fragments with relatively rigid structures, the benzthiazole ring (fragment I), the benzene ring (fragment II), and the dimethylamino group

(fragment III). It was shown²⁹ that photophysical properties of ThT were mainly determined by mutual orientation of fragments I and II, i.e., by torsional angle φ between benzthiazole and benzene rings.

Using ab initio methods, it was established that ThT conformation corresponding to the energy minimum in the ground S_0 state was not planar. Benzthiazole (fragment I) and benzene (fragment II) rings are twisted along C6–C12 bond and torsion angle between their planes is equal to $\varphi \sim 37^\circ$ (Figure 2). The energy barrier for rotation of the fragments I and II along the C6–C12 bond is relatively low, $\Delta E \sim 1200\text{--}1500 \text{ cm}^{-1}$ (RHF/6-31G).

It should be noted that although the barriers on $E_{S_0}(\varphi)$ profile at $\varphi = 90^\circ$ and 270° and at $\varphi = 0^\circ$ and 180° have similar magnitude (Figure 2), the nature of their appearance is different. The energy barriers at $\varphi = 90^\circ$ and 270° (twisted conformation of ThT) are caused by the violation of interaction between π -systems of fragments I and (II + III), whereas the barrier at $\varphi = 0^\circ$ and 180° results due to steric interactions of the methyl group of the benzthiazole ring with the hydrogen atoms of the benzene fragment. It is expected that substitution of the methyl group at N5 atom with a hydrogen atom (the case of BTA-2 cation) should produce a molecule with the planar conformation and common π -electron system of the benzthiazole and the benzene rings. Ab initio calculations of BTA-2 cation confirmed this expectation and revealed that for the given case the dependence of energy $E_{S_0}(\varphi)$ on angle φ had only two minima at $\varphi = 0^\circ$ and 180° (i.e., BTA-2 possessed planar conformation), and heights of energy barriers at $\varphi = 90^\circ$ and 270° were equal to $\sim 3600 \text{ cm}^{-1}$ (RHF/6-31G) (see Figure 2).

Quantum-chemical calculations of the ThT properties in the first excited singlet state were carried out using geometries of the conformers in the ground-state S_0 obtained by ab initio methods with basis set 6-31G. The energy $E_{S_1}(\varphi)$ of ThT in the excited S_1^* state (correspondent to the Franck–Condon state of the molecule) was determined as a sum of ThT energy in the ground state, $E_{S_0}(\varphi)$, obtained by the ab initio method and the energy difference between S_0 and S_1^* levels, $\Delta E_{\text{INDO}}(\varphi)$, calculated by the INDO/S method. Dependence of the energy of the Franck–Condon excited state E_{S_1} on angle φ possesses a minimum in the vicinity of $\varphi = 90^\circ$ (Figure 2). It is interesting to compare $E_{S_1}(\varphi)$ dependencies for ThT and BTA-2 molecules. One can observe that energy profile for BTA-2 in the excited S_1^* state has two minima: at $\varphi = 90^\circ$ (similar as for ThT molecule) and at $\varphi = 0^\circ$, indicating that two excited states of different nature (LE and TICT) determine photophysics of the molecule. It seems reasonable that the same picture is peculiar to the case of ThT; however, the minimum in the vicinity of $\varphi = 0^\circ$ is masked due to repulsion of the methyl group of the benzthiazole ring and the hydrogen atoms of the benzene fragment.

It is noteworthy that shapes of the highest occupied molecular orbital (HOMO) and the lowest unoccupied molecular orbital (LUMO) for ThT conformers depend significantly on the angle φ , indicating that localization of electron density on fragments I–III is changed in S_0 and S_1^* states upon rotation of fragments I and II–III around each other.²⁹ The growth of angle φ value from 37° to 90° results in the following changes of the overall benzthiazole (fragment I) charge: increase from $Z = +0.7$ to $+0.8$ in the ground S_0 state and decrease from $Z = +0.3$ to -0.1 in the Franck–Condon S_1^* state. The dipole moment of ThT in the excited S_1^* state also changes significantly upon twisting of the molecule. It grows from 5.4 D ($\varphi = 0^\circ$) to 7.0 D ($\varphi = 37^\circ$) and ~ 14 D ($\varphi = 90^\circ$). This indicates that

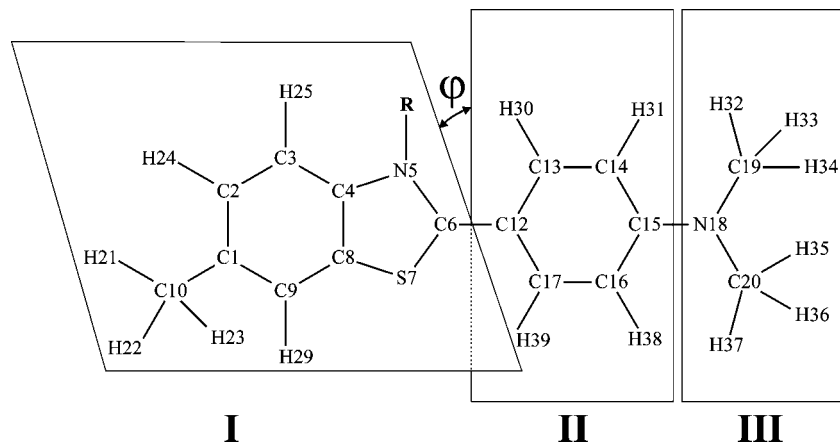


Figure 1. Chemical structure of thioflavin T ($R = \text{CH}_3$) and its derivative BTA-2 ($R = \text{H}$). Three fragments are shown: benzthiazole ring (I), benzene ring (II), and dimethylamino group (III). The torsional angle φ between benzthiazole and benzene rings is indicated.

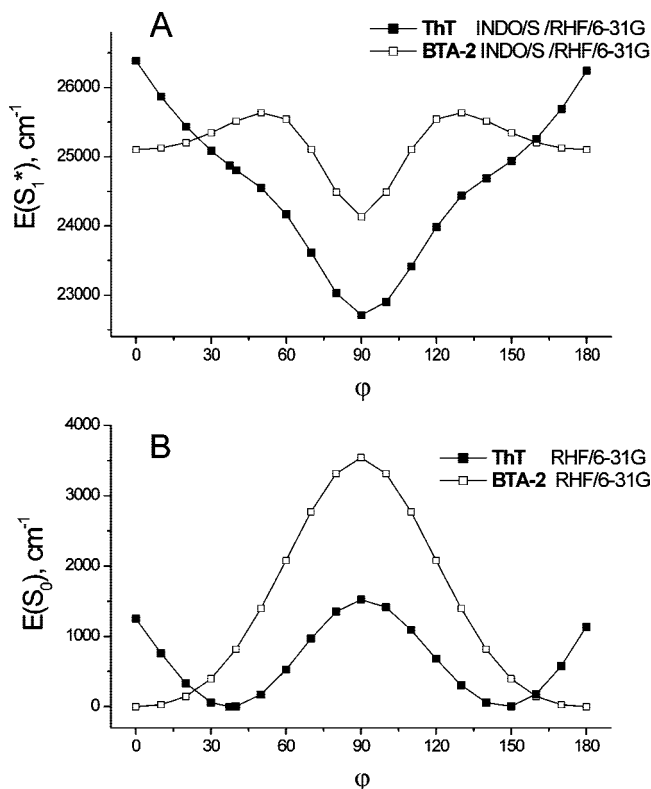


Figure 2. Dependence of ThT and BTA-2 energies in the ground S_0 (B) and Franck–Condon S_1^* state (A) upon φ angle. Calculations were performed with the ab initio method RHF/6-31G. The INDO/S method was used to calculate energies of the excited state. Data points for ThT were taken from ref 29.

intramolecular charge transfer occurs in the excited singlet state S_1^* of ThT upon the change of torsion angle from $\varphi = \varphi_0$ (φ_0 characterize molecule conformation in the S_0 state at the moment of excitation) to 90° , and this process is favorable in energy (Figure 2). The appeared state is a twisted internal charge transfer state (TICT).

Importantly, the overlap area of the HOMO and LUMO is negligible for the twisted conformation of ThT with torsion angle $\varphi = 90^\circ$ or 270° . As a result, the oscillator strength for electron transition between the S_0 and S_1^* states is close to zero for twisted conformation; i.e., TICT state is nonfluorescent since optical transition is forbidden. From the other hand, for torsion angles φ ranging from 0° to 50° oscillator strengths for $S_0 \rightarrow S_1^*$ transition are rather big, ~ 1.0 (the transition dipole moment

is directed along the longest axis of the molecule), and the locally excited (LE) state, corresponding to the above-mentioned torsion angles, is fluorescent. These results of quantum-chemical calculations are crucial for the understanding of the ThT fluorescent properties.

Although the calculations have been carried out for the molecule in gas phase we believe that obtained results will be also relevant to describe photophysics of ThT in polar solvents. Solvent polarity and solute–solvent interactions will influence the energy values due to stabilization of ThT conformers with higher dipole moment. According to calculations, the dipole moment of ThT in the first excited state changes from 5 to 7 D (LE state with torsion angle $\varphi \sim 0^\circ\text{--}37^\circ$) to 14 D (TICT state with $\varphi \sim 90^\circ$). The polar solvent is expected to stabilize twisted conformation of the molecule (i.e., TICT state) to a greater extent than LE state, and one can conclude that $\text{LE} \rightarrow \text{TICT}$ transition accompanied by torsional relaxation is possible for ThT in polar solvents.

Dependence of ThT Fluorescence on Solvent Viscosity and Temperature. Change of solutions viscosity had great effect on ThT fluorescence intensity. Decrease of the glycerol solution viscosity induced by heating or changing water/glycerol ratio was accompanied by dramatic decrease in the fluorescence quantum yield and reduction of the average decay lifetime of the emission (Figure 3, Table 1). Such behavior indicates that a viscosity-dependent nonradiative decay channel exists for the excited state of ThT. We suggest that the deactivation channel is connected with large-amplitude torsional motion in the molecule followed by internal conversion to the ground state, and rate of this process is limited by rotational diffusion of benzthiazole or dimethylaminobenzene rings. Supposing that the rotational diffusion obeys the Debye–Stokes–Einstein (DSE) equation, its rate k_φ should be proportional to the temperature T and inversely proportional to the viscosity η .

$$k_\varphi \sim \frac{T}{\eta} \quad (8)$$

Intersystem crossing to triplet state is usually considered as a major nonradiative deactivation channel for aromatic molecules. However, there is no noticeable phosphorescence for ThT in alcohols or in glycerol at 77 K, and we suggest that conversion to the triplet state may be neglected and the viscosity-dependent torsional relaxation followed by internal conversion is the main nonradiative route of the excited-state deactivation.

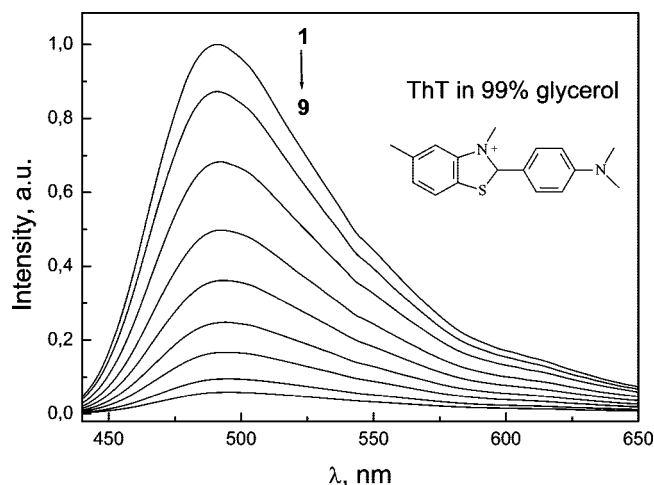


Figure 3. Fluorescence spectra of ThT in 99% glycerol at 284, 287, 292, 297, 302, 307, 312, 323, and 332 K (curves 1–9, respectively). $\lambda_{\text{ex}} = 425$ nm.

TABLE 1: Fluorescence Decay Parameters of ThT in 99% Glycerol at Different Temperatures^a

T, K	τ_1 , ns	S_1	τ_2 , ns	S_2	τ_3 , ns	S_3	$\langle\tau\rangle$, ns	χ^2	DW
77					2.20	1.0	2.20	1.26	1.75
278	0.40	0.34	1.03	0.59	2.07	0.07	0.90	1.08	2.02
289.5	0.33	0.40	0.76	0.60			0.59	1.10	1.78
294	0.34	0.72	0.81	0.28			0.48	1.06	1.78
309	0.14	0.58	0.29	0.44			0.14	1.05	1.81
323	0.12	1.00					0.12	1.11	1.96

^a Multiexponential model was used to describe decay law function $F(t)$. $\lambda_{\text{ex}} = 408$ nm, $\lambda_{\text{em}} = 480$ nm. Uncertainty in lifetime determination was estimated to be ≤ 0.05 ns. DW — Durbin–Watson parameter.

This assumption may be easily checked. Because the fluorescence quantum yield Φ is related to the radiative and nonradiative rate constants by the expression $\Phi = k_r/(k_r + k_{\text{nr}})$ and suggesting that $k_{\text{nr}} \approx k_q$, one can obtain

$$\frac{\Phi}{1 - \Phi} = \frac{k_r}{k_q} \sim \frac{\eta}{T} \quad (9)$$

Linear dependence of $\Phi/(1 - \Phi)$ vs η/T for ThT fluorescence in water/glycerol mixtures (Figure 4A) indicates the applicability of our hypothesis. However, a similar plot for ThT in 99% glycerol (viscosity change was induced by heating) deviates from linearity (Figure 4B), and data points may be fitted using the following equation

$$\frac{\Phi}{1 - \Phi} \sim \left(\frac{\eta}{T}\right)^\alpha \quad (10)$$

with $\alpha = 0.73 \pm 0.02$. The fractional value of α testifies that torsional movement in this case is less affected by friction of surrounding solvent molecules than it is predicted by DSE equation. Indeed, the DSE equation is valid only for rotational diffusion of spherical particle in homogeneous medium with bulk viscosity η , and it fails when sizes of rotating probe moiety and of solvent molecules are comparable. Spatial inhomogeneity and existence of cavities in the solvent, so-called effect of the solvent free volume, must be taken into account.

Comparing behavior of ThT fluorescence in 99% glycerol and water–glycerol mixtures, it must be noted that the rate of torsional relaxation and change of $\Phi/(1 - \Phi)$ value are connected rather with microviscosity η_{micro} but not with macroscopical viscosity η of the solvent. We can only state that linear relationship between η_{micro} and η exists for water/glycerol mixtures. We suppose that free volume effect of the solvent is more pronounced for 99% glycerol; i.e., large enough cavities exist in the solvent, which are comparable in size to ThT fragments. If ThT ring fits into such a cavity, its rotation takes place without significant perturbation of solvent molecules. Therefore, apparent friction experienced by rotating fragments of the dye is diminished. For water–glycerol mixtures the cavities formed by glycerol molecules are filled with water resulting in a more packed net structure of the solvent, and free volume effect seems to be less pronounced.

The empirical relation, similar to eq 10, has been proposed by Loutfy and Arnold³¹ to describe fluorescence quantum yield dependence of *p*-(dialkylamino)benzylidenemalononitrile dyes on bulk viscosity in highly viscous solvents or in polymers above the glass transition temperature. Theoretical explanations of this fact were proposed by Förster and Hoffmann⁵⁵ and later by Sumi^{56,57} on the basis of the two-reaction-coordinate model of Sumi and Marcus, originally developed for electron-transfer reactions. Besides the *p*-(dialkylamino)benzylidenemalononitrile compound, the same dependence on bulk viscosity was observed for triphenylmethane dyes,^{58–62} auramine O,^{63–65} and other molecules generally known as molecular rotors;^{31–36,66–68} i.e., molecules whose fragments rotated relative to each other in the excited state, resulting in the increase of the internal conversion rate.

It is noteworthy that photophysical properties of ThT are very similar to the properties of 9-dicyanovinyljulolidine (DCVJ) considered as a prototypic molecular rotor.³¹ This dye is also characterized by low quantum yield to triplet state, and the main routes of its excited-state deactivation are radiative transition and isomerization process along vinyl bond.³⁴ Dependence of fluorescence quantum yield on viscosity for DCVJ solution in glycerol was reported to obey eq 10 with $\alpha = 0.75$.³¹ Moreover, DCVJ was proposed as a fluorescent probe alternative to ThT for detection of amyloid fibrils, especially on early stages of their formation.³⁰

Our results indicate that ThT exhibits fluorescent properties typical for molecular rotors, and its photophysics may be reasonably described by two competing deactivation pathways: (1) fluorescence emission and (2) torsional relaxation, leading to internal conversion to the ground state.

Consider dependence of ThT fluorescence parameters on temperature in more detail. Radiation lifetime $\tau_r = 3.4$ ns for ThT in glycerol was determined from the relationship $\tau_r = 1/k_r = \langle\tau\rangle/\Phi$ using experimental data about average decay lifetime $\langle\tau\rangle$ and quantum yield Φ of the emission. Heating of ThT solution in 99% glycerol from 283 to 323 K resulted in growth of the nonradiative transition rate k_q from 1.1×10^9 to 14.3×10^9 s^{−1}. It is noteworthy that in the studied temperature range mainly nonradiative transition determines ThT lifetime in the excited state because radiative transition rate $k_r = 1/\tau_r = 0.3 \times 10^9$ s^{−1} is much smaller.

Analyzing the temperature dependence of the ThT fluorescence, it is important to remember that increase of temperature has also effect on solvent viscosity, and this relation may be described by the following equation:³¹

$$\eta^{-1} = \eta_0^{-1} \exp(-\Delta E(\eta)/k_B T) \quad (11)$$

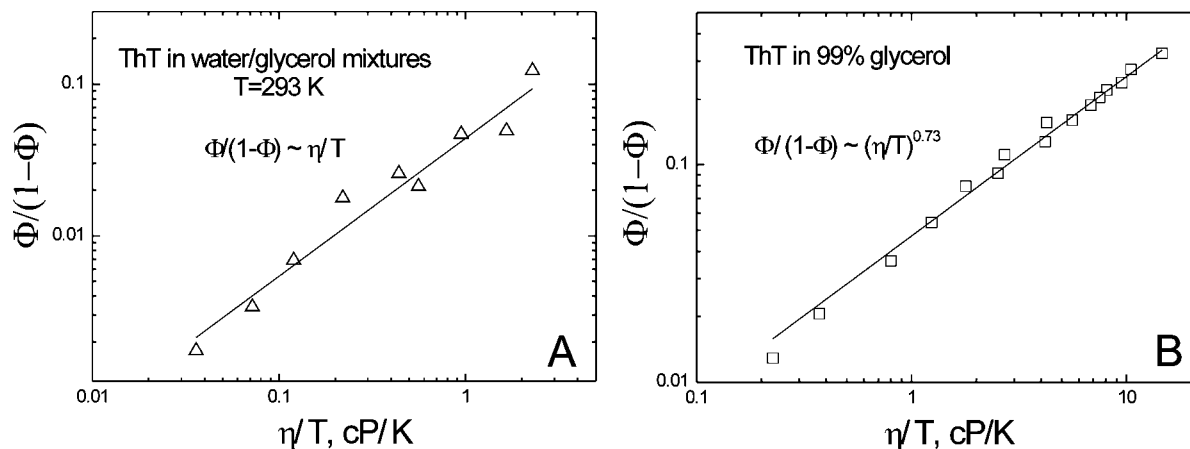


Figure 4. Dependence of $\Phi/(1 - \Phi)$ vs (η/T) for ThT in water–glycerol mixture at 293 K (A) and in 99% glycerol at different temperatures (B). $\lambda_{\text{ex}} = 425$ nm.

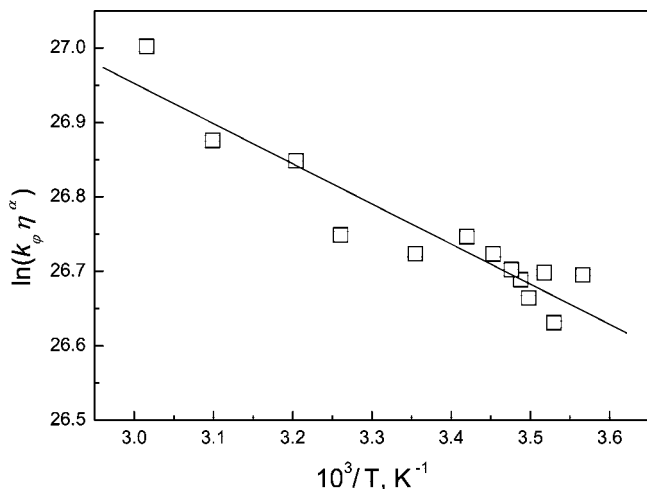


Figure 5. Dependence of $\ln(k_\phi \eta^\alpha)$ vs $1/T$ for ThT in 99% glycerol.

where $\Delta E(\eta)$ is the activation energy of the viscous flow of the solvent. Using the data about dependence of 99% glycerol viscosity upon temperature,³⁷ $\Delta E(\eta)$ was found to be $5170 \pm 130 \text{ cm}^{-1}$.

It was shown³⁴ that viscosity effects on torsional motion for molecular rotors may be taken into account, and one can obtain activation energy of internal rotation $\Delta E(\varphi)$ from the equation

$$k_\varphi = \frac{\nu}{\eta^\alpha} \exp\left(-\frac{\Delta E(\varphi)}{k_B T}\right) \quad (12)$$

where ν is the limiting pressure exerted by the rotor and α the coefficient from (10) which describes frictional forces between rotor and surrounding solvent.

Fitting the experimental data (Figure 5) with the use of eq 12, it was found that $\Delta E(\varphi)$ has a very low value of only $370 \pm 100 \text{ cm}^{-1}$. It is noteworthy that estimated energy barrier for ThT rings twisting is comparable to the energy of thermal motion kT ($\sim 210 \text{ cm}^{-1}$ at 300 K). Therefore, we may conclude that the rate of torsional relaxation of the ThT fragments in the excited state, leading to charge transfer and nonradiative deactivation, is mainly determined by solvent viscosity.

Time-Resolved Fluorescence of ThT in Glycerol. Steady-state fluorescence data predict that the value of fluorescence decay lifetime τ must strongly depend upon viscosity of medium, i.e., mobility of ThT fragments relative to each other.

To prove this, we have analyzed the dependence of the fluorescence decay of ThT in glycerol on temperature.

In order to work with high emission intensities, the 99% glycerol was used, and temperature was changed from 278 to 323 K (Table 1). At first, the multiexponential model (eq 3) was used to represent the decay law function $F(t)$. Measurements of time-resolved fluorescence revealed that ThT fluorescence decay is complex and can be described using at least three ($T = 278$ K) or two exponential components (289.5–309 K). Only for the solution at 323 K a monoexponential decay was observed with short lifetime of ~ 0.1 ns. It is possible that in this case decay kinetics is also more complex; however, insufficient time resolution of the fluorescence spectrometer prevents us to detect this.

Consider possible reasons of nonexponentiality for ThT fluorescence decay. First of all, multiexponential character of the fluorescence decay kinetics may be caused by heterogeneity of the dye molecules in the ground or excited states.

It was reported that ThT was able to form dimers⁶⁹ in water near freezing point at 273 K when ThT concentration is more than 10^{-4} M. In particular, dimerization of ThT resulted in appearance of a new absorption band at 390 nm. In present work all measurements were performed using the ThT solutions with concentrations of 10^{-5} – 10^{-6} M to prevent formation of dimers or aggregates. Shapes of the absorption spectra were constant, proving that no ThT dimers were formed under the conditions used in this study. Probability of the excimer formation^{22,24} for viscous diluted solutions of ThT is negligible, especially taking into account the short lifetime of the ThT molecules in the excited state. Furthermore, we cast doubt the ability of ThT to form dimers or excimers earlier due to electrostatic repulsion of ThT cations and showed that the use of ThT solutions with high concentration and therefore high optical densities led to some erroneous conclusions about ThT spectral properties.²⁸

It is widely known that incomplete solvent or dye structure relaxation may result in nonexponential character of fluorescence decay. The data of steady-state measurements indicate that structural heterogeneity of ThT molecules arisen from torsional motion in the excited state can be the principal factor that influences the fluorescence decay. Nonequilibrium process of torsional movements of molecular fragments as well as incomplete solvent relaxation²⁶ will result in inability to adequately describe ThT emission decay curves using the multiexponential model. It is more natural to describe the fluorescence decay of such set of molecules by continuous lifetime distribution of emitting centers.

TABLE 2: Fluorescence Decay Parameters of ThT in 99% Glycerol at Different Temperatures^a

<i>T</i> , K	τ_0 , ns	σ^2 , ns ²	$\langle\tau\rangle$, ns	χ^2
77	2.2	<0.001	2.2	1.30
278	0.92	0.25	1.1	1.16
289.5	0.40	0.07	0.6	1.19
294	0.31	0.07	0.5	1.15
309	0.10	<0.01	0.1	1.34

^a Lifetime distribution model was used to describe decay law function $F(t)$. $\lambda_{\text{ex}} = 408$ nm, $\tau_{\text{em}} = 480$ nm. Uncertainty in lifetime determination was estimated to be ≤ 0.05 ns. Average decay lifetime was calculated by the following expression $\langle\tau\rangle = (\int \alpha(\tau)\tau^2 d\tau) / (\int \alpha(\tau)\tau d\tau)$.

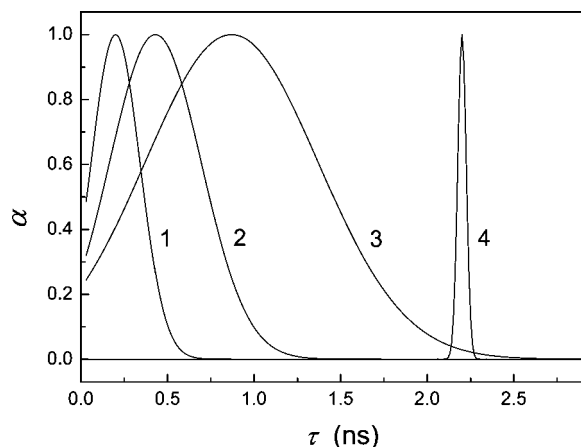


Figure 6. Fluorescence lifetime distribution for ThT in 99% glycerol. Curves 1, 2, 3, and 4 correspond to 300, 289.5, 278, and 77 K, respectively. $\lambda_{\text{ex}} = 408$ nm, $\lambda_{\text{em}} = 480$ nm.

To explore this possibility, the experimental fluorescence decay curves were analyzed using the lifetime distributions model. Lifetime distribution for ThT was represented in a form of a truncated Gaussian function (see Materials and Methods). Table 2 shows the results of this analysis and illustrates that the lifetime distribution for glycerol solution of ThT in temperature range 278–309 K may be satisfactorily described by a single Gaussian function. Data for temperatures above 309 K are not shown as considerable (more than 10-fold) decrease in the duration of the fluorescence decay takes place under these conditions, and reconstruction of lifetime distribution may be not reliable. Table 2 and Figure 6 show that positions of the maxima of distributions (τ_0) and their variances (σ^2) change significantly upon temperature growth. The largest average lifetime of fluorescence decay $\langle\tau\rangle \sim 2.2$ ns was observed for ThT in 99% glycerol at 77 K (it coincides with τ_0 value). For this case the lifetime distribution is very narrow (see Table 2); i.e., fluorescence decay is virtually monoexponential. The increase in the temperature of the glycerol solution resulted in decrease of τ_0 value. Temperature growth was also accompanied by monotonous change of σ^2 values, and the maximal value was observed at $T = 278$ K. Such behavior can be explained assuming that σ^2 represents a measure of ThT molecules heterogeneity in the excited state due to incomplete torsional and solvent relaxation.

In highly viscous solutions (for example, in glycerol or *n*-propanol at 77 K, i.e., under conditions that could be considered as limiting case of the viscous solvent) where $k_r \gg k_q$, and therefore, τ is close to radiative lifetime value ($\tau_r = 3.4$ ns) and quantum yield is maximal, the lifetime distribution of emitting molecules $\alpha(\tau)$ is narrow, and fluorescence decay is

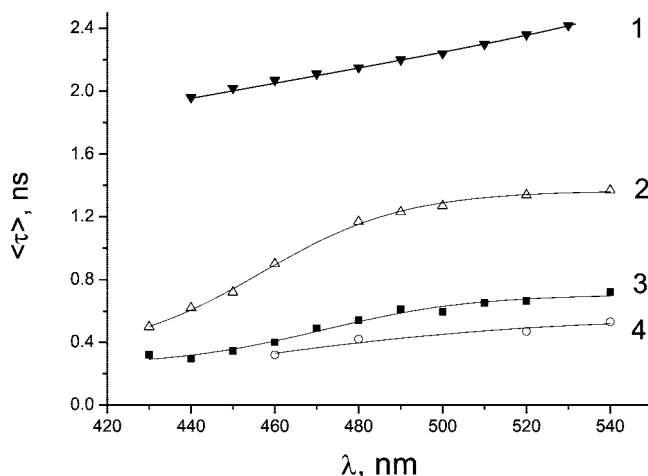


Figure 7. Dependence of the averaged fluorescence decay lifetime $\langle\tau\rangle$ for ThT in 99% glycerol on emission wavelength at 77 K (1), 278 K (2), 294 K (3), and 296 K (4).

practically monoexponential (Table 1, Figure 6). It is interesting to note that in spite of rigid environment of glassy matrix fluorescence decay lifetime of ThT is ~ 1.5 times shorter than τ_r . Similar behavior was reported³⁴ for DCVJ in ethanol at 77 K and explained by nonrigid fixation of the rotor molecule in the glassy matrix where rotation was only partially hindered by contact with surrounding molecules. We suggest that this explanation is also relevant to the case of ThT; i.e., torsional relaxation is not completely blocked in the glassy matrix of glycerol at 77 K.

In the cases when k_r and k_q are comparable (for example ThT in glycerol at 278 K has $k_r = 0.3 \times 10^9$ s⁻¹ and $k_q = 0.8 \times 10^9$ s⁻¹) the fluorescence kinetics of ThT has complicated nonexponential behavior, and $\alpha(\tau)$ distribution is strongly broadened. In solvents with low viscosity ($k_r \ll k_q$) the quenching process due to the torsional relaxation is more efficient, and the center of lifetime distribution is shifted to smaller values and the distribution becomes again more narrow.

For ThT in glycerol at room temperature the noticeable changes (2–3-fold) in the mean fluorescence lifetime occur within the frames of fluorescence spectrum (Figure 7). Furthermore, the position of the fluorescence spectrum depends on temperature and the “red-edge excitation effect” was observed (data not shown). Therefore, ThT in glycerol behaves as typical system with inhomogeneous broadening of the fluorescence spectrum when values of k_q , k_r , and solvent relaxation rate k_{solv} are comparable.

Interestingly, despite the noticeable changes in the mean fluorescence lifetime within the ThT fluorescence spectrum in 99% glycerol at $T = 293$ K, the polarization degree remains constant and high (Figure 8). Change of glycerol solution viscosity from 1200 to 120 cP did not alter the high polarization degree of ThT fluorescence ($P = 0.45$), although ~ 5 -fold decrease in intensity was observed. This phenomenon confirms nonequilibrium character of the emission from LE state and can be explained taking into account the fact that rotational correlation time ρ of the whole ThT molecule is greater than the time needed for torsional relaxation of the ThT fragments which is associated with TICT state formation and the radiationless deactivation process. Although the reliable data about polarization degree were obtained only for relatively viscous media, we suppose that the same behavior is also valid for ThT in low-viscosity solvents. Furthermore, quantum-chemical calculations showed that the transition dipole moment is directed

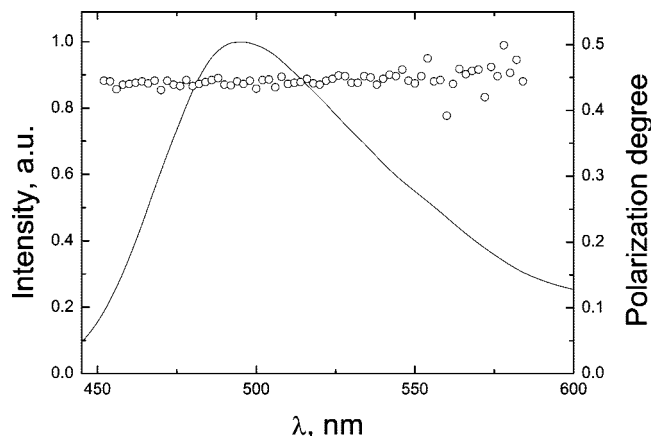


Figure 8. Variation of polarization degree (circles) across the emission spectrum (solid line) of ThT in 99% glycerol at $T = 293$ K. $\lambda_{\text{ex}} = 425$ nm.

along the longest axis in ThT molecule, and its orientation does not depend on the torsion angle φ between the benzothiazole and aminobenzene rings. The following possible scenario for ThT molecules may be proposed: after photoexcitation the transition dipole moment of ThT does not have time to significantly change its orientation during the excited-state lifetime since motion of the whole ThT molecule cannot compete with the rings twisting process. Experimental data in stretched polymer films⁷⁰ that report about orientation of transition dipole moment along the long axis of ThT support our findings.

TICT-State Formation as a Reason for Viscosity-Dependent Nonradiative Deactivation of ThT Excited State. Our results indicate that photophysics of ThT may be reasonably described by two competing deactivation pathways: (1) fluorescence emission from LE state and (2) effectively barrierless intramolecular charge transfer process between fluorescent LE and nonfluorescent TICT states accompanied by twisting of molecular fragments.

In low-viscosity solvents the rate of LE \rightarrow TICT transition process may effectively compete with radiative and other nonradiative transitions from LE state to the ground state. Blocking of ThT fragments rotation must lead to suppression of LE \rightarrow TICT transition and increase of fluorescence quantum yield. This behavior is typical to so-called molecular rotors,^{31–36,66–68} molecules that undergo twisted internal charge-transfer process. Fluorescence properties of molecular rotors were thoroughly analyzed in several studies.^{31,34}

Two possible schemes of excited-state deactivation for molecular rotors were discussed elsewhere.^{63–65,71} According to the first model,⁷¹ temporal dependence of population distribution along the excited-state energy surface was modeled using the modified Smoluchowski diffusion equation. It was assumed that barrierless excited-state potential surface had a position-dependent sink, responsible for nonradiative transition to the ground state. As soon as a molecule reached the sink position (twisted conformation in our case), very fast nonradiative transition occurred. In the alternative model⁶³ it was proposed that not the growth of nonradiative but decrease of the radiative transition rate explained fluorescence quenching for twisted conformation (TICT state).

We suggest that the latter model is more relevant to describe ThT photophysics. Let us consider probable changes in ThT geometry following photoexcitation and transition to the excited Franck–Condon state S_1^* . If we assume that energy profile of

relaxed ThT molecule in the excited-state S_1 is approximately similar to the dependence of Franck–Condon S_1^* state energy vs angle φ (Figure 2), then geometry relaxation of ThT in the excited state will lead to the twisted conformation, i.e., torsion angle φ will change from $\varphi = \varphi_0$ (initial conformation, correspondent to S_0 state) to 90° (TICT state with the twisted rings). Naturally, relaxation process affects not only torsion angle φ value but also other geometry parameters of ThT denoted by ω (bond lengths, angles, etc.). However, the rotation of the molecular fragments relative to each other requires more time than the time needed to alter bond lengths or angles (i.e., set of parameters ω) determining the configuration of the ThT fragments; therefore, we may distinguish two relaxation processes. The first, relatively fast, process is associated with the changes in the set of parameters ω from ω_0 (relevant to S_0 state) to ω_1 (relevant to S_1 state), and the second, essentially slower, process is due to the changes in the torsion angle φ accompanied by intramolecular charge transfer.

On the basis of quantum-chemical calculations the following model of ThT excited-state deactivation is suggested. Immediately after the transition to Franck–Condon state S_1^* the molecule is characterized by geometrical parameters $\varphi = \varphi_0$ and $\omega = \omega_0$. Fast vibrational relaxation of the ω parameters leads to the locally excited (LE) state S_1 ($\varphi = \varphi_0$, $\omega = \omega_1$) which is capable to fluoresce (oscillator strength is about 1.0). Then much slower relaxation process takes place leading to the nonfluorescent TICT state with $\varphi \sim 90^\circ$ and $\omega = \omega_1$. According to calculations, there is no energy barrier between LE and TICT states or this barrier is very low. Experimental studies of ThT fluorescence in glycerol reveal that internal rotation of ThT fragments in the excited state is actually barrierless and fully determined by dye microviscosity. Blocking of the torsional relaxation process (for instance, by change of viscosity or rigidity of microenvironment) will increase the probability of photon emission from LE state and will result in a growth of fluorescence quantum yield of ThT.

Results of our study provide an explanation for the dramatic (more than 3 orders of magnitude) increase in ThT quantum yield upon incorporation of the dye into amyloid-like fibrils. We suggest that this effect is determined by the steric hindrance of the internal rotation of the ThT aromatic rings relative to each other which blocks transition to nonfluorescent TICT state.

The data obtained support the model of ThT incorporation into the amyloid fibrils proposed by Krebs et al.⁷⁰ The authors of this work draw attention that the side chains of amino acid residues on each side of the β -sheet form neat rows, running in the direction of the β -sheet, and resulting in “channels” in between every other row. They also showed that the free space of these “channels” suits for only one molecule of ThT. Getting into the channel ThT appears to be closely surrounded by the side chains of residues forming β -sheets, which results in restriction of intramolecular twisting process of ThT rings after photoexcitation of the dye. As we have shown growth of viscosity (or rigidity) of ThT microenvironment leads to blocking of TICT process and significant increase of fluorescence quantum yield. We believe that exactly this feature of photophysics allowed the use of ThT for the determination of amyloid fibrils.

Conclusions

Our data show that photoinduced TICT process in the excited state accompanied by torsional relaxation of the aromatic rings is the major reason for the quenching of ThT fluorescence in solutions with low viscosity. Intramolecular

charge transfer results in transition from highly fluorescent LE state to nonfluorescent TICT state, and reaction coordinate of this process can be associated with torsional angle φ between benzothiazole and benzene rings. TICT state corresponds to ThT conformation with twisted rings ($\varphi = 90^\circ$). Experimental investigations and ab initio calculations revealed that TICT process in the excited state is actually barrierless, and its rate is fully determined by solvent viscosity or rigidity of microenvironment. On the basis of these data, it is concluded that ThT belongs to the class of molecular rotors.

Because of the fact that torsional and solvent relaxation rates for ThT in glycerol are comparable, the dye fluorescence is nonequilibrium and has an inhomogeneously broadened spectrum, and emission kinetics is significantly nonexponential. The nonequilibrium character of ThT fluorescence from LE state results also in anomalously high polarization degree of emission ($P = 0.45$) in solvents of different viscosity due to the fact that rotational correlation time of the whole ThT molecule is considerably greater than the fluorescence decay lifetime.

Results of our study provide an explanation for the dramatic (more than 3 orders of magnitude) increase in ThT quantum yield upon incorporation of the dye into amyloid-like fibrils. This effect is determined by the steric hindrance of the internal rotation of the ThT aromatic rings relative to each other which block transition to nonfluorescent TICT state.

Acknowledgment. This work was supported in part by Belarusian Republican Foundation for Fundamental Research (Grants F06-351, X06P-115, X08P-217, B08P-216), Russian Foundation of Basic Research (Grants 08-04-90052, 07-04-01454), Program "Leading Scientific Schools of Russia" (Grant #1961.2008.4), Program "Molecular and Cell Biology" RAS.

References and Notes

- (1) Harper, J. D.; Lieber, C. M.; Lansbury, P. T. *Chem. Biol.* **1997**, *4*, 951–959.
- (2) Kelly, J. W. *Structure* **1997**, *5*, 595–600.
- (3) Carrell, R. W.; Goopu, B. *Curr. Opin. Struct. Biol.* **1998**, *8*, 799–809.
- (4) Hashimoto, M.; Masliah, E. *Brain Pathol.* **1999**, *9*, 707–720.
- (5) Koo, E. H.; Lansbury, P. T., Jr.; Kelly, J. W. *Proc. Natl. Acad. Sci. U.S.A.* **1999**, *96*, 9989–9990.
- (6) Uversky, V. N.; Talapatra, A.; Gillespie, J. R.; Fink, A. L. *Med. Sci. Monitor* **1999**, *5*, 1001–1012.
- (7) Uversky, V. N.; Talapatra, A.; Gillespie, J. R.; Fink, A. L. *Med. Sci. Monitor* **1999**, *5*, 1238–1254.
- (8) Naiki, H.; Higuchi, K.; Hosokawa, M.; Takeda, T. *Anal. Biochem.* **1989**, *177*, 244–249.
- (9) Naiki, H.; Higuchi, K.; Matsushima, K.; Shimada, A.; Chen, W. H.; Hosokawa, M.; Takeda, T. *Lab. Invest.* **1990**, *62*, 768–773.
- (10) LeVine, H., III. *Protein Sci.* **1993**, *2*, 404–410.
- (11) LeVine, H., III. *Amyloid: Int. J. Exp. Clin. Invest.* **1995**, *2*, 1–6.
- (12) LeVine, H., III. *Arch. Biochem. Biophys.* **1997**, *342*, 306–316.
- (13) LeVine, H., III. *Methods Enzymol.* **1999**, *309*, 274–284.
- (14) Allsop, D.; Swanson, L.; Moore, S.; Davies, Y.; York, A.; El-Agnaf, O. M.; Soutar, I. *Biochem. Biophys. Res. Commun.* **2001**, *285*, 58–63.
- (15) Yoshiike, Y.; Chui, D. H.; Akagi, T.; Tanaka, N.; Takashima, A. *J. Biol. Chem.* **2003**, *278*, 23648–23655.
- (16) Goers, J.; Permyakov, S. E.; Permyakov, E. A.; Uversky, V. N.; Fink, A. L. *Biochemistry* **2002**, *41*, 12546–12551.
- (17) Ban, T.; Hamada, D.; Hasegawa, K.; Naiki, H.; Goto, Y. *J. Biol. Chem.* **2003**, *278*, 16462–16465.
- (18) Kumita, J. R.; Weston, C. J.; Choo-Smith, L. P.; Woolley, G. A.; Smart, O. S. *Biochemistry* **2003**, *42*, 4492–4498.
- (19) Zhu, L.; Zhang, X. J.; Wang, L. Y.; Zhou, J. M.; Perrett, S. J. *Mol. Biol.* **2003**, *328*, 235–254.
- (20) Hawe, A.; Sutter, M.; Jiskoot, W. *Pharm. Res.* **2008**, *25*, 1487–1499.
- (21) Raj, C. R.; Ramaraj, R. *Photochem. Photobiol.* **2001**, *74*, 752–759.
- (22) Ilanchelian, M.; Ramaraj, R. *J. Photochem. Photobiol. A: Chem.* **2004**, *162*, 129–137.
- (23) Groenning, M.; Olsen, L.; van de Weert, M.; Flink, J. M.; Frokjaer, S.; Jorgensen, F. S. *J. Struct. Biol.* **2007**, *158*, 358–369.
- (24) Raj, C. R.; Ramaraj, R. *Chem. Phys. Lett.* **1997**, *273*, 285–290.
- (25) Khurana, R.; Coleman, C.; Ionescu-Zanetti, C.; Carter, S. A.; Krishna, V.; Grover, R. K.; Roy, R.; Singh, S. J. *Struct. Biol.* **2005**, *151*, 229–238.
- (26) Maskevich, A. A.; Stsiapura, V. I.; Kuzmitsky, V. A.; Kuznetsova, I. M.; Povarova, O. I.; Uversky, V. N.; Turoverov, K. K. *J. Proteome Res.* **2007**, *6*, 1392–1401.
- (27) Friedhoff, P.; Schneider, A.; Mandelkow, E. M.; Mandelkow, E. *Biochemistry* **1998**, *37*, 10223–10230.
- (28) Voropai, E. S.; Samstov, M. P.; Kaplevskii, K. N.; Maskevich, A. A.; Stepuro, V. I.; Povarova, O. I.; Kuznetsova, I. M.; Turoverov, K. K.; Fink, A. L.; Uversky, V. N. *J. Appl. Spectrosc.* **2003**, *70*, 868–874.
- (29) Stsiapura, V. I.; Maskevich, A. A.; Kuzmitsky, V. A.; Turoverov, K. K.; Kuznetsova, I. M. *J. Phys. Chem. A* **2007**, *111*, 4829–4835.
- (30) Lindgren, M.; Sorgjerd, K.; Hammarstrom, P. *Biophys. J.* **2005**, *88*, 4200–4212.
- (31) Loutfy, R. O.; Arnold, B. A. *J. Phys. Chem.* **1982**, *86*, 4205–4211.
- (32) Loutfy, R. O. *Pure Appl. Chem.* **1986**, *58*, 1239–1248.
- (33) Haidekker, M. A.; Brady, T. P.; Lichtlyer, D.; Theodorakis, E. A. *Bioorg. Chem.* **2005**, *33*, 415–425.
- (34) Allen, B. D.; Benniston, A. C.; Harriman, A.; Rostron, S. A.; Yu, C. *Phys. Chem. Chem. Phys.* **2005**, *7*, 3035–3040.
- (35) Valeur, B. *Molecular Fluorescence: Principles and Applications*; Wiley-VCH: New York, 2001.
- (36) Haidekker, M. A.; Theodorakis, E. A. *Org. Biomol. Chem.* **2007**, *5*, 1669–1678.
- (37) Segur, J. B. Physical properties of glycerol and its solutions. In *Glycerol*; Miner, C. S., Dalton, N. N., Eds.; Reinhold Publ. Corp.: New York, 1953; pp 238–334.
- (38) Jones II, G.; Jackson, W. R.; Choi, C.; Bergmark, W. R. *J. Phys. Chem.* **1985**, *89*, 294–300.
- (39) Stepuro, V. I. *Vestn. Grodno State Univ.* **2001**, *1*, 52–61.
- (40) Marquardt, D. W. *J. Soc. Ind. Appl. Math.* **1963**, *11*, 431–441.
- (41) O'Connor, D. V.; Phillips, D. *Time-Related Single Photon Counting*; Academic Press: New York, 1984.
- (42) James, D. R.; Ware, W. R. *Chem. Phys. Lett.* **1986**, *126*, 7–11.
- (43) Alcalá, J. R.; Gratton, E.; Prendergast, F. G. *Biophys. J.* **1987**, *51*, 925–936.
- (44) McWhirter, J. G.; Pike, E. R. *J. Phys. A: Math. Gen.* **1978**, *11*, 1729–1745.
- (45) Gryczynski, I.; Johnson, M. L.; Lakowicz, J. R. *Biophys. Chem.* **1994**, *52*, 1–13.
- (46) Maskevich, A. A.; Artsukevich, I. M.; Stepuro, V. I. *J. Mol. Struct.* **1997**, *408/409*, 261–264.
- (47) Tichonov, A.; Arsenin, V. *Solutions of Ill-posed Inverse Problems*; John Wiley & Sons: London, 1977.
- (48) Maskevich, A. A.; Basharin, S. K.; Gachko, G. A.; Kivach, L. N.; Maskevich, S. A. *J. Appl. Spectrosc.* **1990**, *53*, 1022–1027.
- (49) Basharin, S. K.; Gachko, G. A.; Kivach, L. N.; Maskevich, S. A.; Maskevich, A. A.; Udovychenko, V. P. *J. Appl. Spectrosc.* **1990**, *52*, 48–52.
- (50) Grinvald, A.; Steinberg, I. Z. *Anal. Biochem.* **1974**, *59*, 583–598.
- (51) Zerner, M. C.; Loew, G. H.; Kirchner, R. F.; Mueller-Westerhoff, U. T. *J. Am. Chem. Soc.* **1980**, *102*, 589–599.
- (52) Nemukhin, A. V.; Grigorenko, B. L.; Granovsky, A. A. *Moscow Univ. Chem. Bull.* **2004**, *45*, 75.
- (53) Schmidt, M. W.; Baldridge, K. K.; Boatz, J. A.; Elbert, S. T.; Gordon, M. S.; Jensen, J. H.; Koseki, S.; Matsunaga, N.; Nguyen, K. A.; Su, S.; Windus, T. L.; Dupuis, M.; Montgomery, J., Jr. *J. Comput. Chem.* **1993**, *14*, 1347–1363.
- (54) Portmann, S.; Luthi, H. P. *Chimia* **2000**, *54*, 766–770.
- (55) Forster, T.; Hoffmann, G. Z. *Phys. Chem.* **1971**, *65*, 63–76.
- (56) Sumi, H. *J. Phys. Chem.* **1991**, *95*, 3334–3350.
- (57) Sumi, H. *J. Mol. Liq.* **2001**, *90*, 185–194.
- (58) Ben-Amotz, D.; Harris, C. B. *J. Chem. Phys.* **1987**, *86*, 4856–4870.
- (59) Ben-Amotz, D.; Harris, C. B. *J. Chem. Phys.* **1987**, *86*, 5433–5440.
- (60) Ben-Amotz, D.; Jeanloz, R.; Harris, C. B. *J. Chem. Phys.* **1987**, *86*, 6119–6127.
- (61) Brey, L. A.; Schuster, G. B.; Drickamer, H. G. *J. Chem. Phys.* **1977**, *67*, 2648–2650.
- (62) Mokhtari, A.; Fini, L.; Chesnoy, J. J. *J. Chem. Phys.* **1987**, *87*, 3429–3435.
- (63) van der Meer, M. J.; Zhang, H.; Glasbeek, M. J. *J. Chem. Phys.* **2000**, *112*, 2878–2887.
- (64) Glasbeek, M.; Zhang, H. *Chem. Rev.* **2004**, *104*, 1929–1954.
- (65) Glasbeek, M.; Zhang, H.; Chagnenet, P.; Plaza, P.; Martin, M. M.; Rettig, W. Femtosecond studies of Intramolecular Bond Twisting in

Solution. In *Femtochemistry*; de Schryver, F. C., Feyter, S., Schweitzer, G., Eds.; Wiley: Weinheim, Germany, 2001; pp 417–430.

(66) Loutfy, R. O.; Law, K. Y. *J. Phys. Chem.* **1980**, *84*, 2803–2808.

(67) Law, K. Y.; Loutfy, R. O. *Macromolecules* **1981**, *14*, 587–591.

(68) Kung, C. E.; Reed, J. K. *Biochemistry* **1989**, *28*, 6678–6686.

(69) Schirra, R. *Chem. Phys. Lett.* **1985**, *119*, 463–466.

(70) Krebs, M. R.; Bromley, E. H.; Donald, A. M. *J. Struct. Biol.* **2005**, *149*, 30–37.

(71) Bagchi, B.; Fleming, G. R.; Oxtoby, D. W. *J. Chem. Phys.* **1983**, *78*, 7375–7385.

JP805822C